Electronic Supporting Information

Cyclometalated iridium complexes based on monodentate aminophosphanes

Marco Palmese, Jesús J. Pérez-Torrente, and Vincenzo Passarelli*

Departamento de Química Inorgánica, Instituto de Síntesis Química y Catálisis Homogénea (ISQCH), Universidad de Zaragoza-CSIC, C/ Pedro Cerbuna 12, ES-50009 Zaragoza.

1. Crystal structure of $6PF_6$ and $12PF_6$

Figure SI1-top shows the asymmetric unit in the crystal structure of **6**PF_6. Two of the cations $[IrH\{\kappa^2 C,P\text{–}SiMe_3N(4\text{-}C_6H_3CH_3)PPh_2\}(cod)(CH_3CN)]^+$ exhibit *A* configuration (Figure SI1-bottom) of the metal centre (Ir1 and Ir3), whereas *C* configuration (Figure SI1-bottom) is observed for the remaining two cations (Ir2 and Ir4).

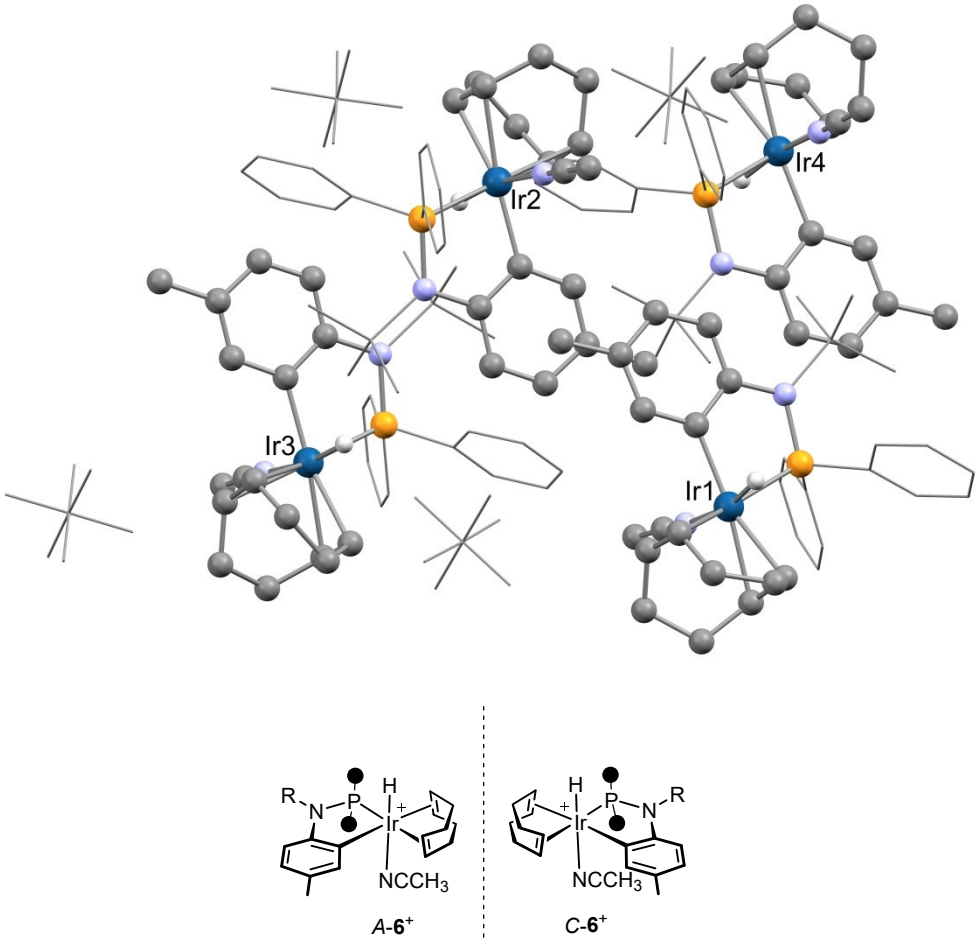

Fig. SI1. (top) View of the asymmetric unit in the crystal structure of **6**PF_6. For clarity, most hydrogen atoms are omitted and a wireframe style is adopted for the phenyl groups, the $SiMe_3$ moiety and the hexafluorophoshate anions; (bottom) View of the *C* and *A* enantiomers of $\mathbf{6}^+$.

Figure SI2 shows the asymmetric unit in the crystal structure of **12**PF_6. One of the cations $[IrH\{\kappa^2 C,P\text{–}SiMe_3N(4\text{-}C_6H_3CH_3)PPh_2\}(HNP)_2(CH_3CN)]^+$ exhibits *C* configuration of the metal centre (Ir1), whereas *A* configuration is observed for the remaining cation (Ir2).

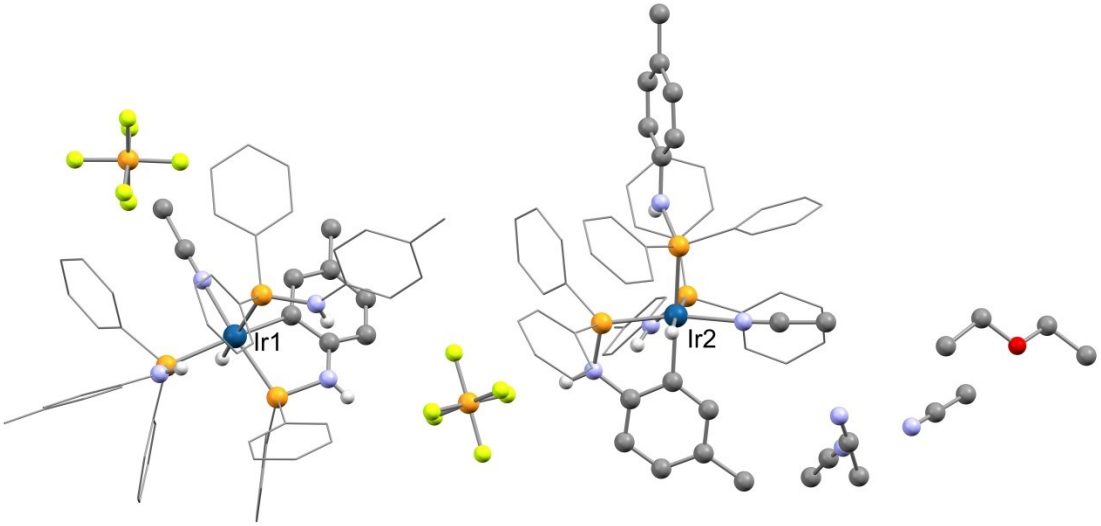

Fig. SI2. View of the asymmetric unit in the crystal structure of **12**PF_6. For clarity, most hydrogen atoms are omitted and a wireframe style is adopted for phenyl and selected tolyl groups.

2. IR spectrum of 4[$IrCl_2(CO)_2$] in CH_2Cl_2

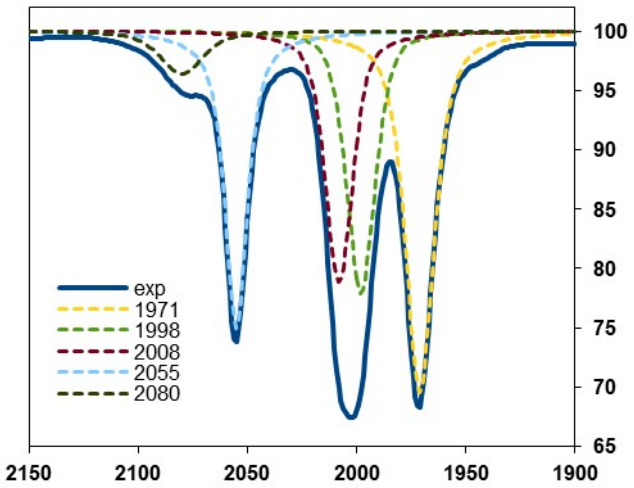

Fig. SI3. IR spectrum of **4**[$IrCl_2(CO)_2$] in CH_2Cl_2 and its deconvolution.

3. Polyhedral symbols for I, II, 5^+, IV^+, V^+, 12^+ and 13^+.

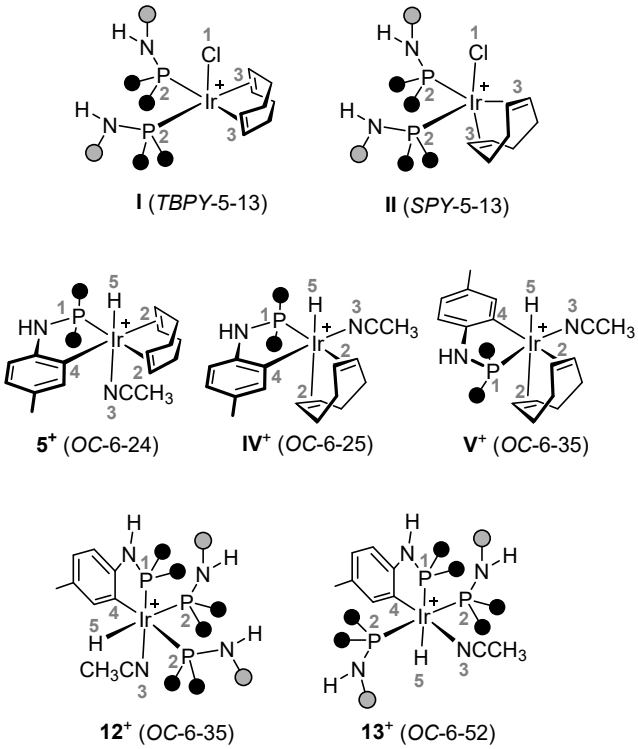

Fig. SI4. Polyhedral symbols and ligand priority labelling scheme for **I**, **II**, $\mathbf{5}^+$, $\mathbf{IV}^+$, $\mathbf{V}^+$, $\mathbf{12}^+$ and $\mathbf{13}^+$.

4. Selected NMR data for 1, 2, 5⁺, 6⁺, 10⁺, 12⁺, and 13⁺, with the proposed assignment

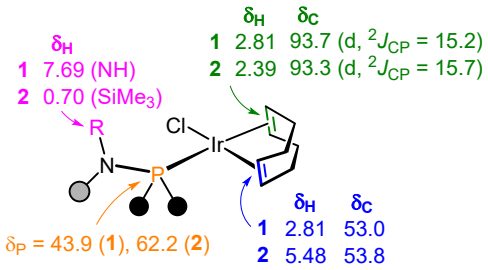

Fig. SI5. Selected NMR data for **1** and **2** and the proposed assignment (δ are given in ppm, *J* in Hz).

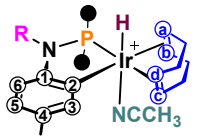

5⁺, R = H
6⁺, R = $SiMe_3$

P	δ_P
5⁺	62.5
6⁺	73.9

NR	δ_H
5⁺	5.22 (NH)
6⁺	0.14 ($SiMe_3$)

IrH	δ_H (J_{HP})
5⁺	-16.07 (d, 10.6)
6⁺	-16.43 (d, 11.2)

tol	δ_H [5⁺/6⁺]	δ_C (J_{CP}) [5⁺/6⁺]
1	-/-	150.8 (d, 17.2)/154.5 (d, 16.2)
2	-/-	121.2 (d, 2.8)/126.8 (d, 3.5)
3	6.70/6.72	134.4/135.4
4	-/-	129.9/130.2
5	6.83/6.91	126.6/125.9
6	6.88/7.14	110.7 (d, 14.4)/114.1 (d, 16.1)

cod	δ_H [5⁺/6⁺]	δ_C (J_{CP}) [5⁺/6⁺]
a	5.77/5.54	92.11/94.6
b	5.40/5.37	92.06/93.9
c	4.76/4.69	99.8 (d, 10.5)/100.8 (d, 10.6)
d	4.61/4.09	98.0 (d, 12.8)/100.4 (d, 12.2)

Fig. SI6. Selected NMR data for **5⁺** and **6⁺** and the proposed assignment (δ are given in ppm, *J* in Hz).

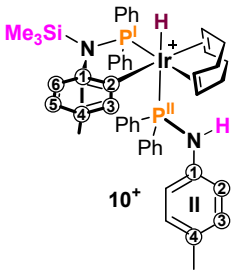

	δ_P (J_{PP})
P^I	66.6 (d, 22.2)
P^{II}	1.22 (d, 22.2)

	δ_H (J_{HP})
IrH	-10.18 (dd, 105.5, 12.4)
NH	4.81 (d, 17.0)
Me^{Si}	0.25 (d, 18.2)

II	δ_H	δ_C (J_{CP})
1	-	138.9 (d, 10.6)
2	5.77	117.9 (d, 5.0)
3	6.60	129.2
4	-	128.7
Me	2.03	20.4

I	δ_H	δ_C (J_{CP})
1	-	154.4 (d, 16.0)
2	-	124.4 (dd, 13.4, 10.3)
3	6.14	136.0
4	-	130.17
5	6.95	127.0
6	7.19	116.5 (d, 16.0)
Me	2.20	20.6

Fig. SI7. Selected ^1H, ^{13}C and ^{31}P NMR data of **10⁺** with the proposed assignment (δ are given in ppm, *J* in Hz).

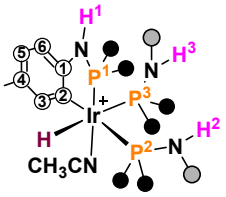

12⁺

	δ_H (J_{HP})
IrH	-11.83 (dt, 150.5, 16.2)
NH^1	6.28
NH^2	5.17 (d, 19.6)
NH^3	4.64 (d, 18.5)

	δ_P (J_{PP})
P^1	49.8 (t, 11.5)
P^2	19.8 (dd, 16.0, 11.5)
P^3	11.2 (dd, 16.0, 11.5)

	δ_H	δ_C (J_{CP})
1	-	149.8 (dd, 14.3, 2.1)
2	-	126.0 (d, 4.9)
3	6.38	137.9 (dd, 2.6, 0.9)
4	-	129.8
5	6.81	127.0 (d, 1.5)
6	6.87	112.2 (d, 14.0)
Me	2.10	21.4

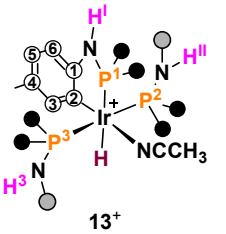

13⁺

	δ_H (J_{HP})
IrH	-9.86 (dt, 133.0, 18.6)
NH^1	5.71 (d, 2.2, NH^I)
$NH^{2/3}$	5.18 (t, 8.3, NH^{II})

	δ_P (J_{PP})
P^1	43.4 (t, 16.0)
$P^{2/3}$	19.7 (d, 11.5)

	δ_H	δ_C (J_{CP})
1	-	152.0 (d, 22.0)
2	-	113.4 (td, 10.0, 1.6)
3	6.23	145.0
4	-	not observed
5	6.78	129.9 (d, 1.2)
6	6.94	111.7 (d, 13.4)
Me	1.95	21.3

Fig. SI8. Selected ^{1}H, ^{13}C and ^{31}P NMR data for **12⁺** and **13⁺** with the proposed assignment (δ are given in ppm, *J* in Hz).

5. ^{1}H, $^{31}P\{^{1}H\}$ and $^{13}C\{^{1}H\}$-APT NMR spectra of $SiMe_3NP$, 1-3, $4[IrCl_2(CO)_2]$, $5PF_6$, $6PF_6$, 9^+, $11PF_6$, $12PF_6$, and $13PF_6$

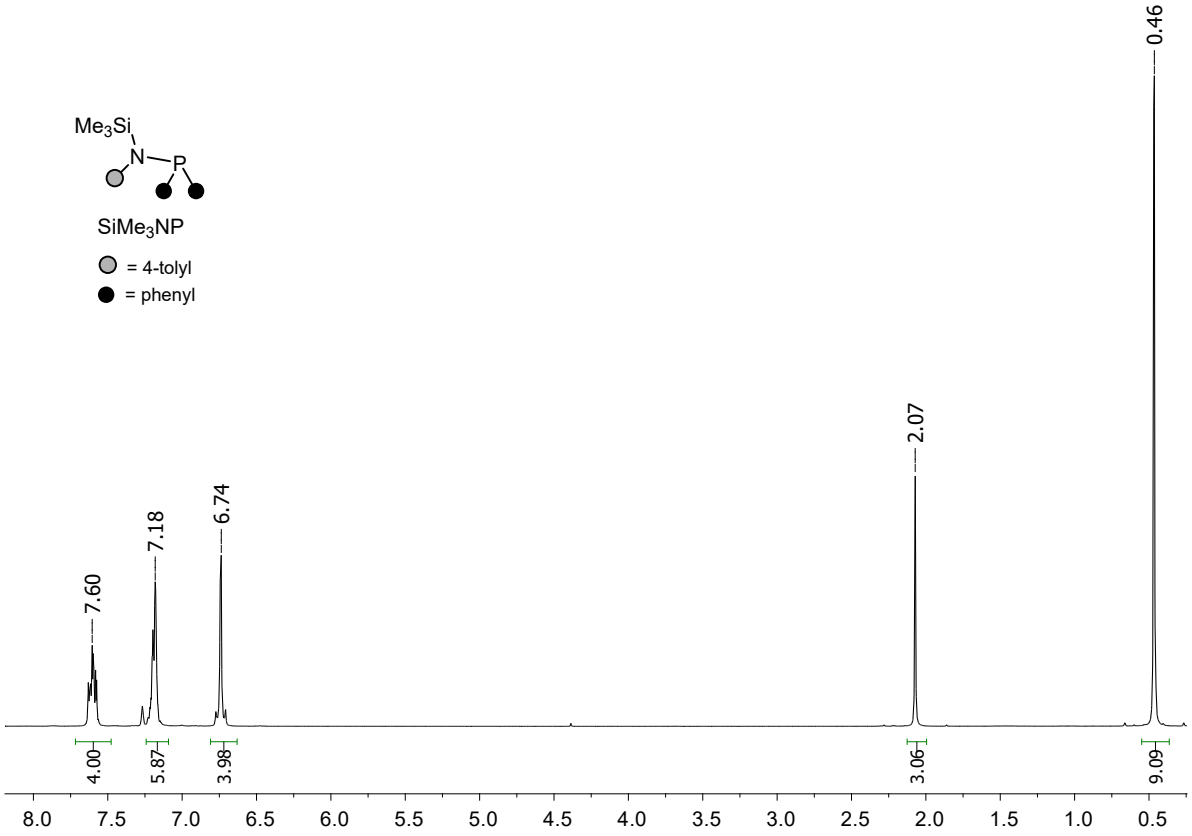

Fig. SI9. ^{1}H NMR spectrum of $SiMe_3NP$.

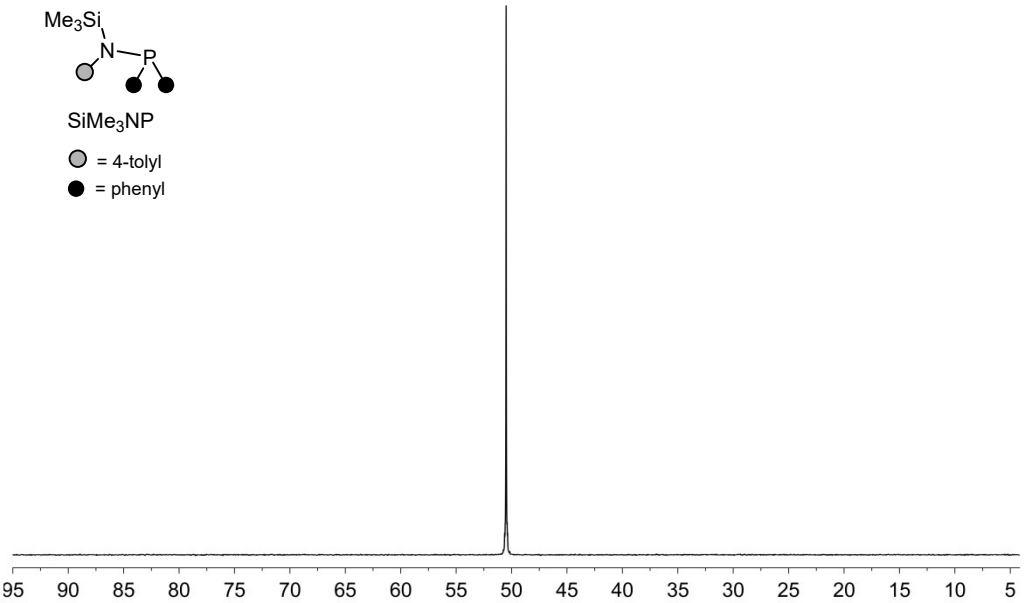

Fig. SI10. $^{31}P\{^{1}H\}$ NMR spectrum of $SiMe_3NP$.

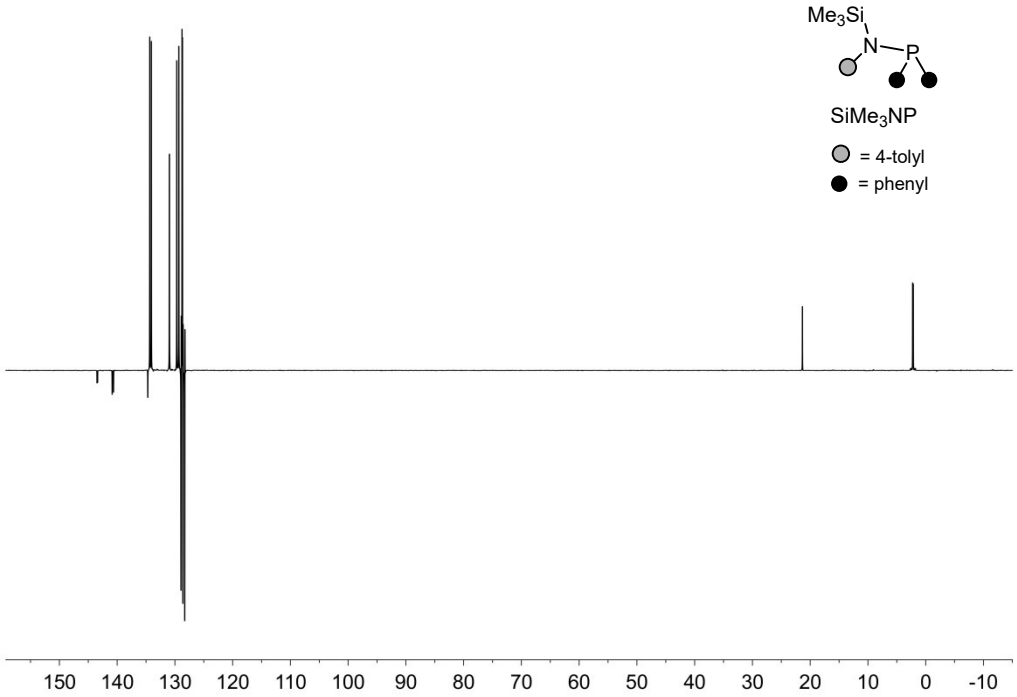

Fig. SI11. $^{13}C\{^{1}H\}$-apt NMR spectrum of $SiMe_3NP$.

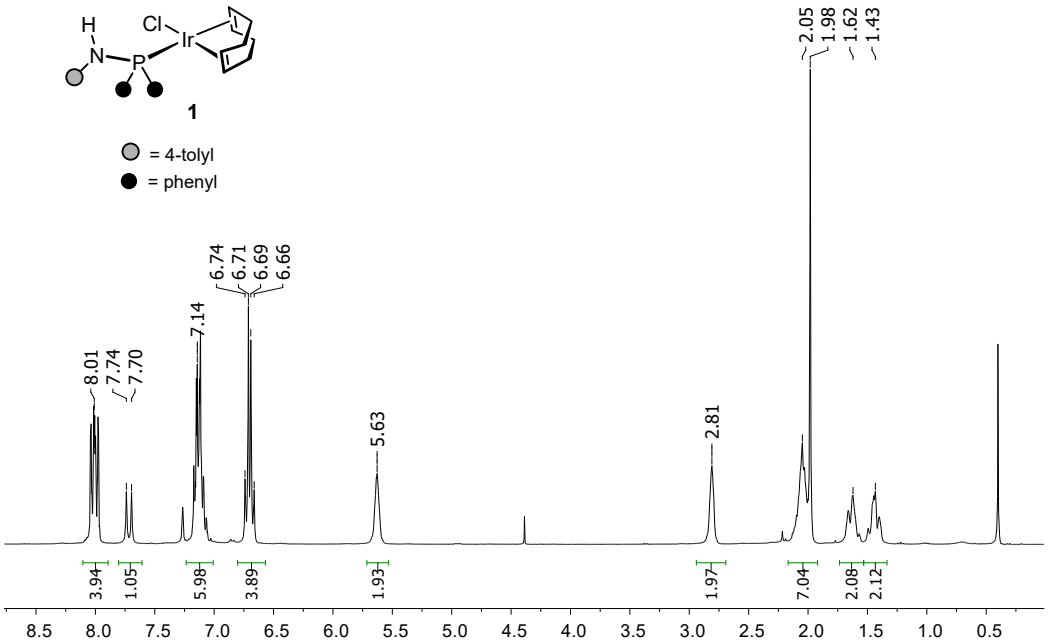

Fig. SI12. ^{1}H NMR spectrum of **1**.

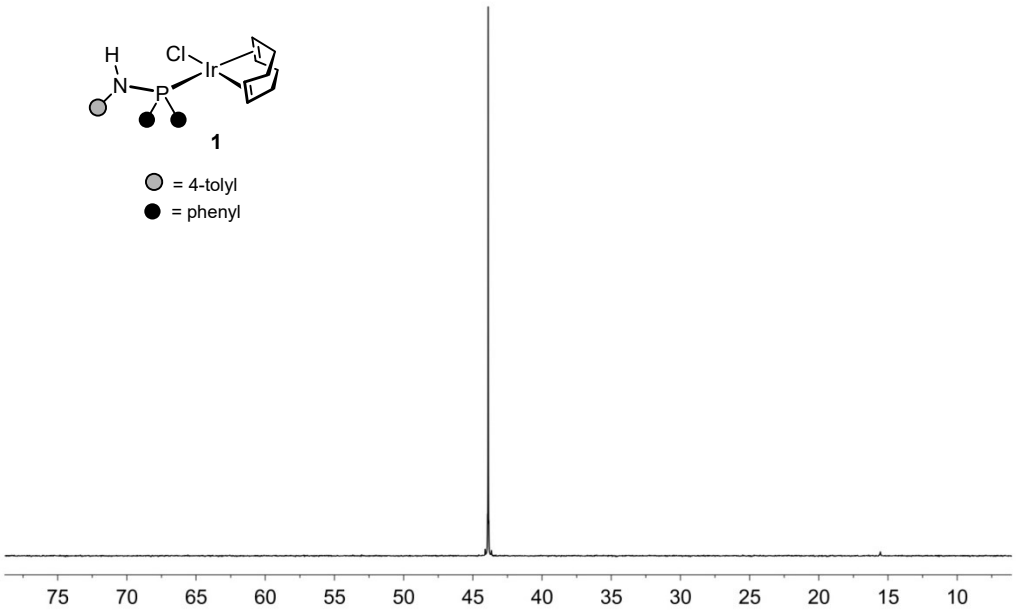

Fig. SI13. $^{31}P\{^{1}H\}$ NMR spectrum of **1**.

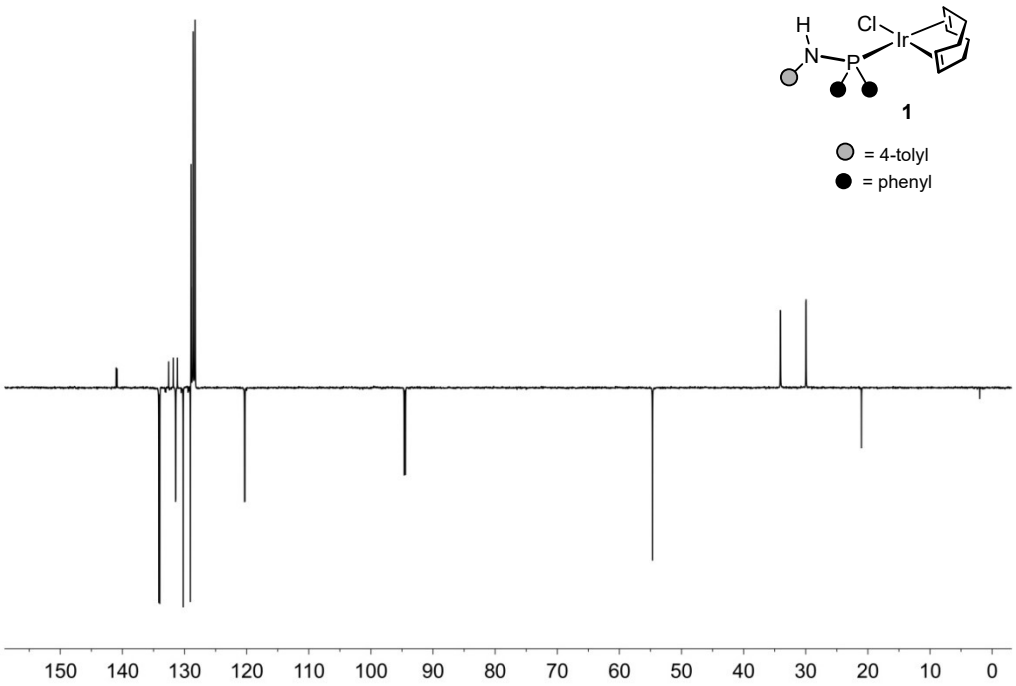

Fig. SI14. $^{13}C\{^{1}H\}$-apt NMR spectrum of **1**.

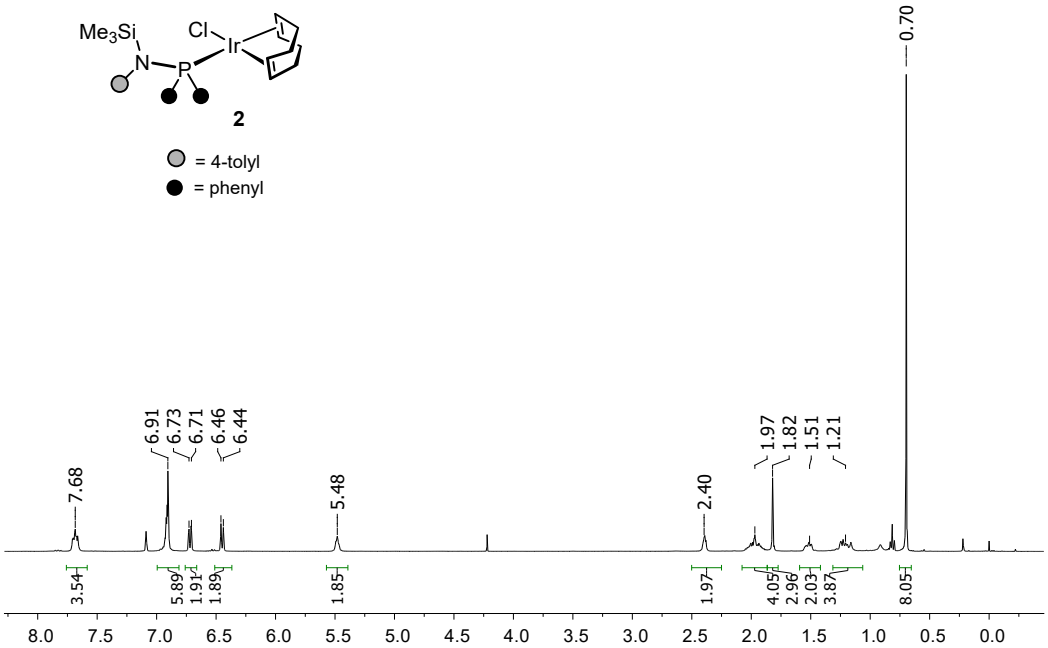

Fig. SI15. ^{1}H NMR spectrum of **2**.

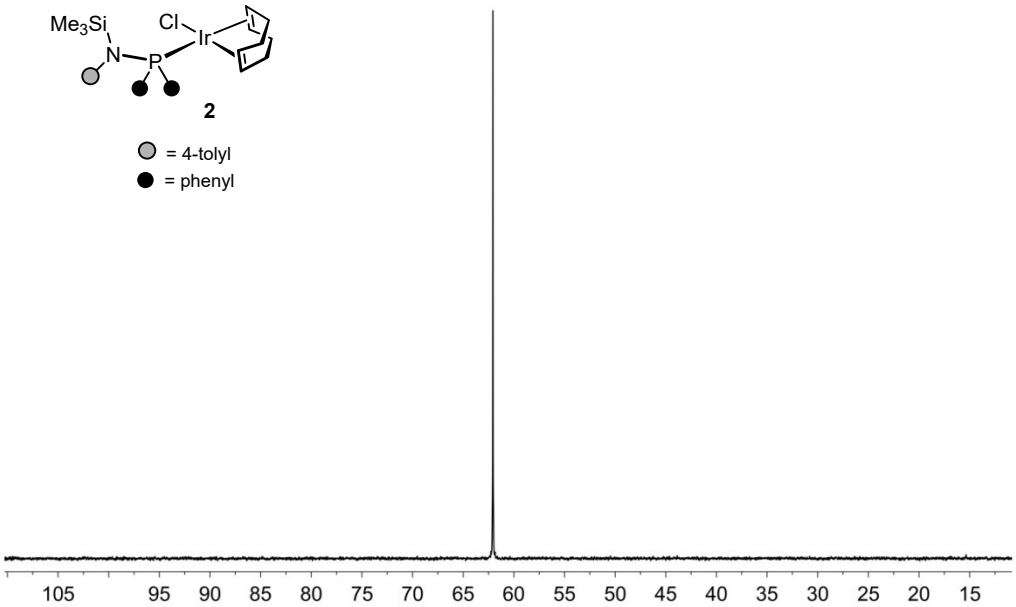

Fig. SI16. ^{31}P{^{1}H} NMR spectrum of **2**.

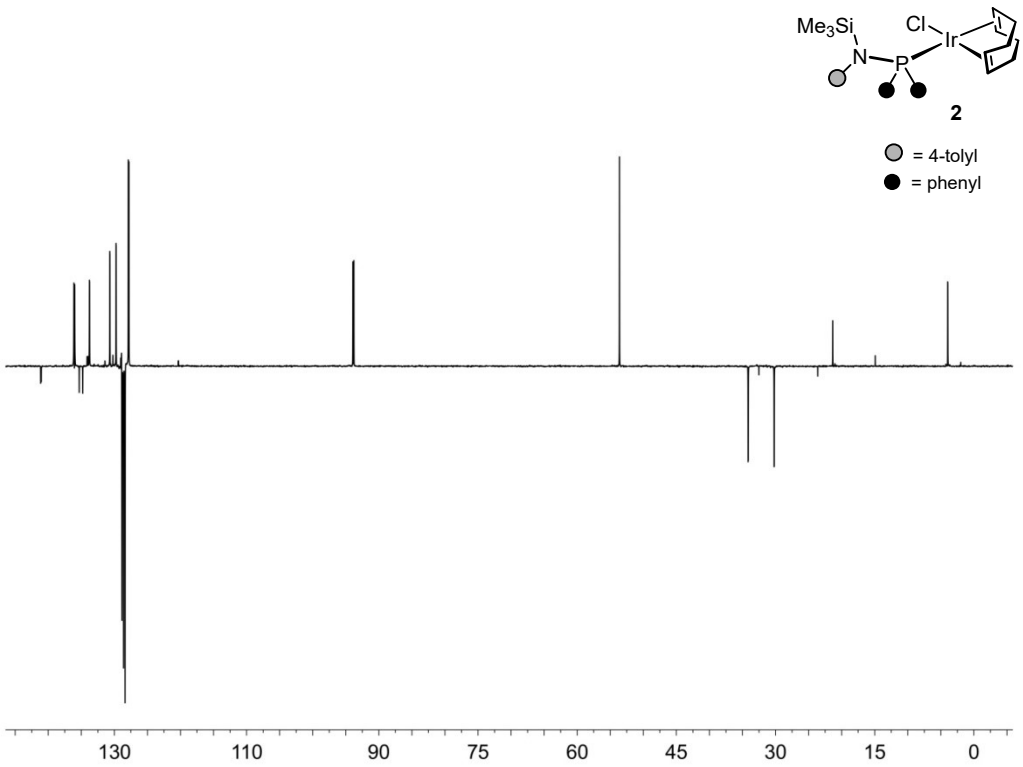

Fig. SI17. $^{13}C\{^{1}H\}$-apt NMR spectrum of **2**.

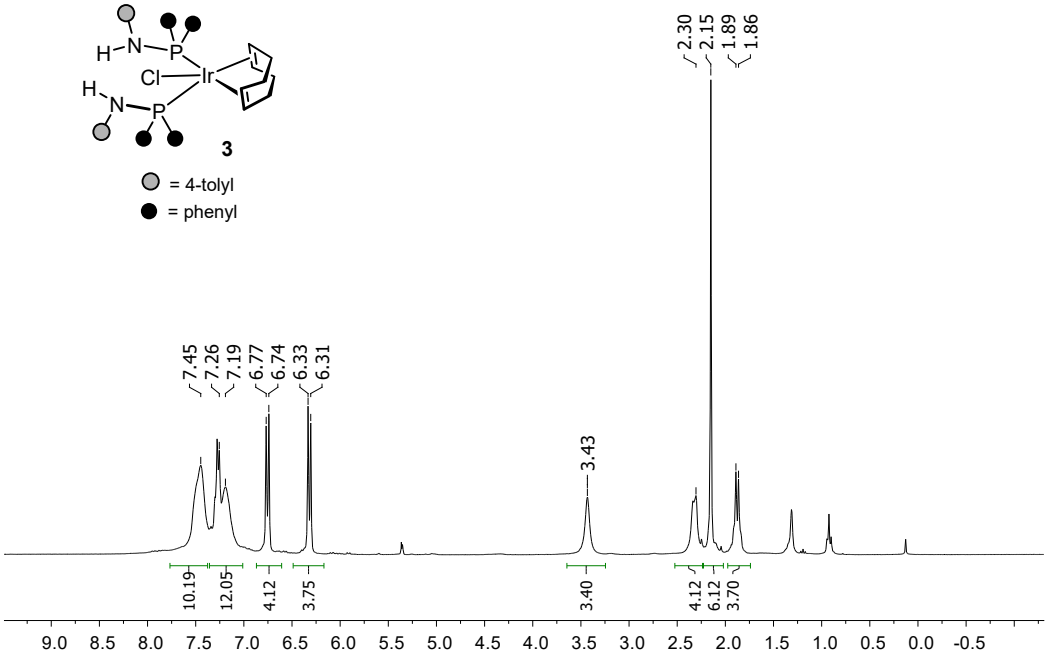

Fig. SI18. ^{1}H NMR spectrum of **3** (298 K).

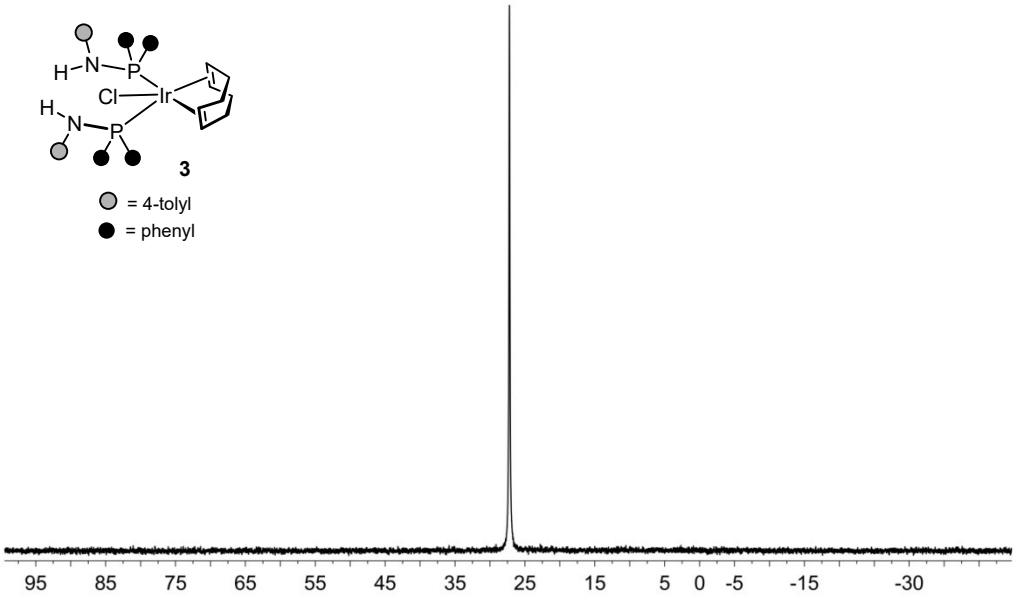

Fig. SI19. $^{31}P\{^{1}H\}$ NMR spectrum of **3** (298 K).

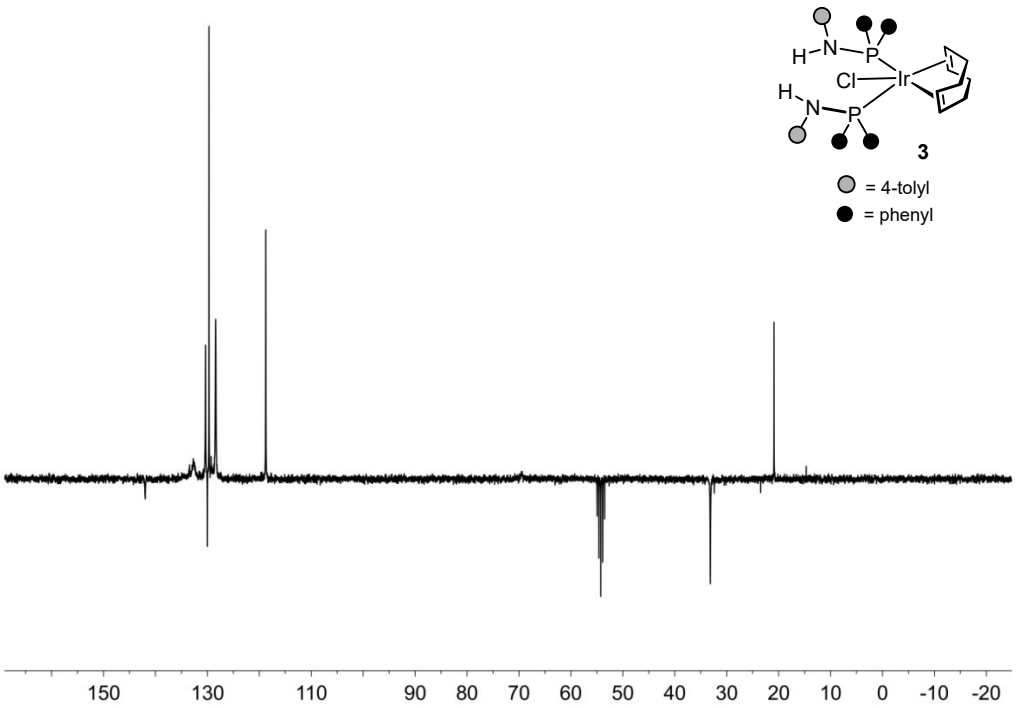

Fig. SI20. $^{13}C\{^{1}H\}$-apt NMR spectrum of **3** (298 K).

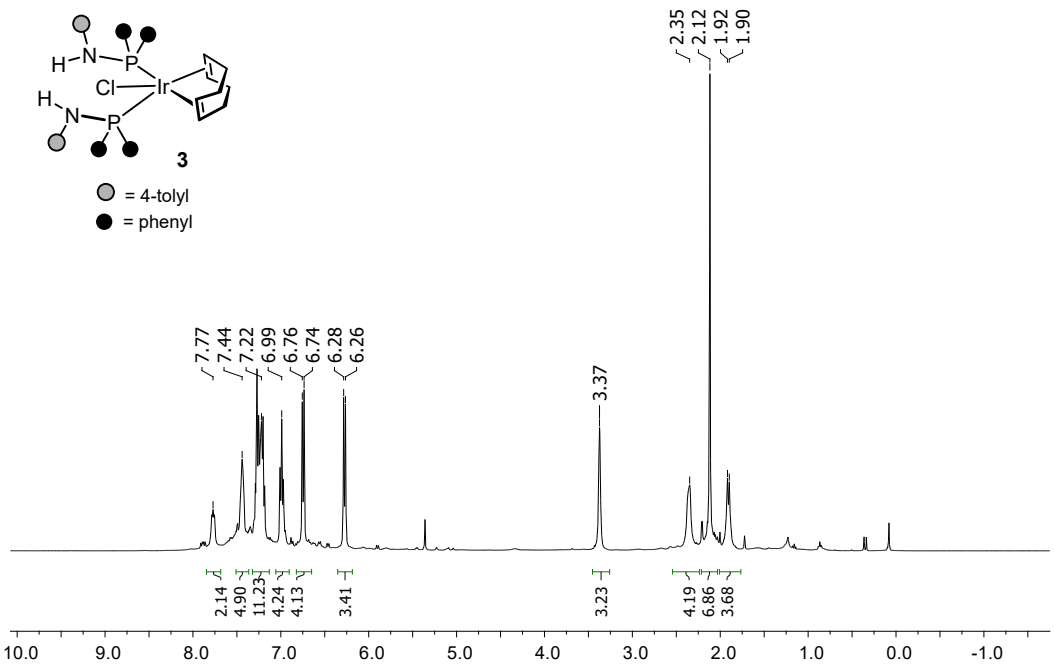

Fig. SI21. ^{1}H NMR spectrum of **3** (213 K).

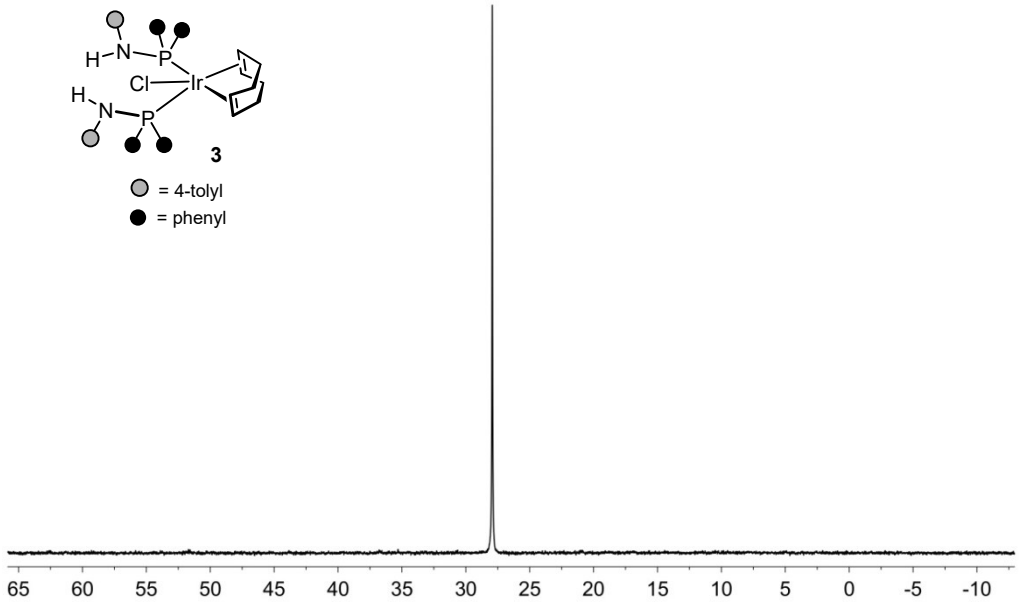

Fig. SI22. ^{31}P{^{1}H} NMR spectrum of **3** (213 K).

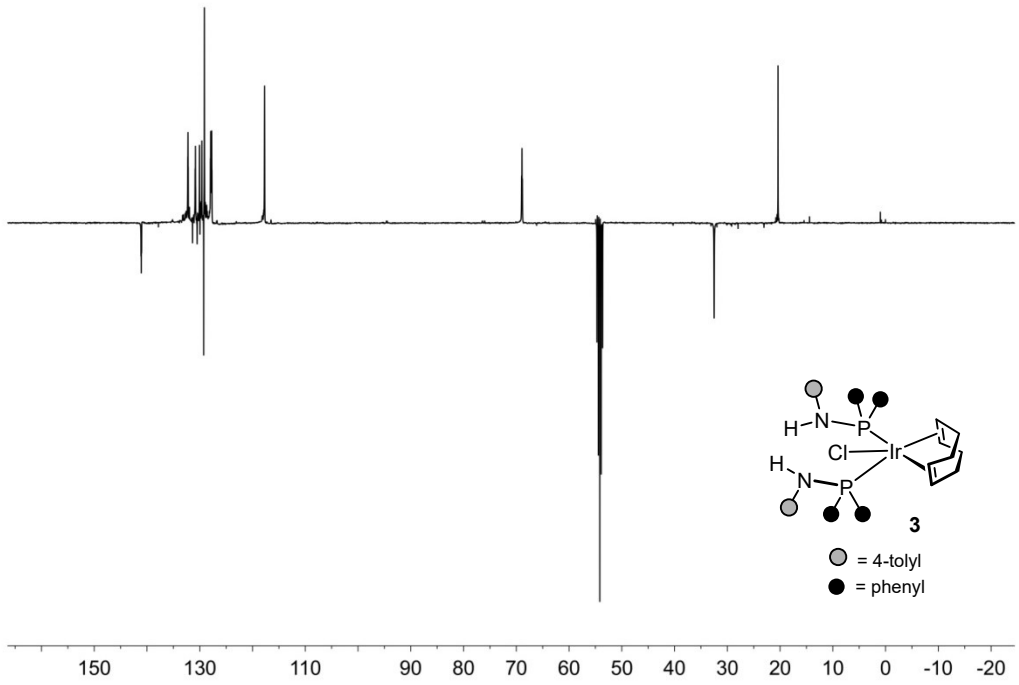

Fig. SI23. $^{13}C\{^{1}H\}$-apt NMR spectrum of **3** (213 K).

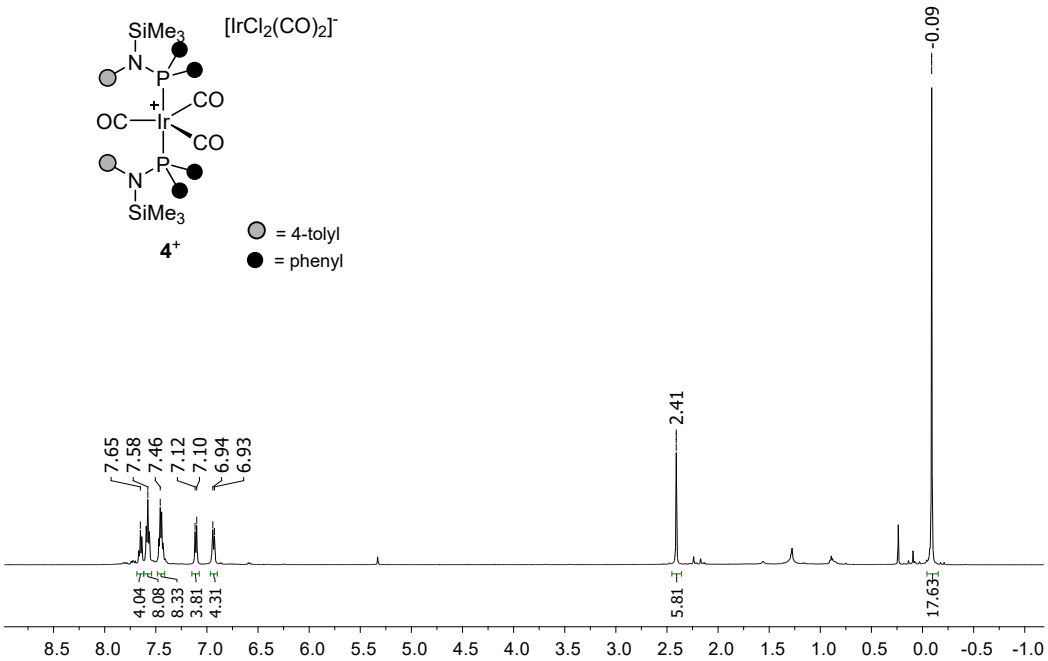

Fig. SI24. ^{1}H NMR spectrum of **4**.

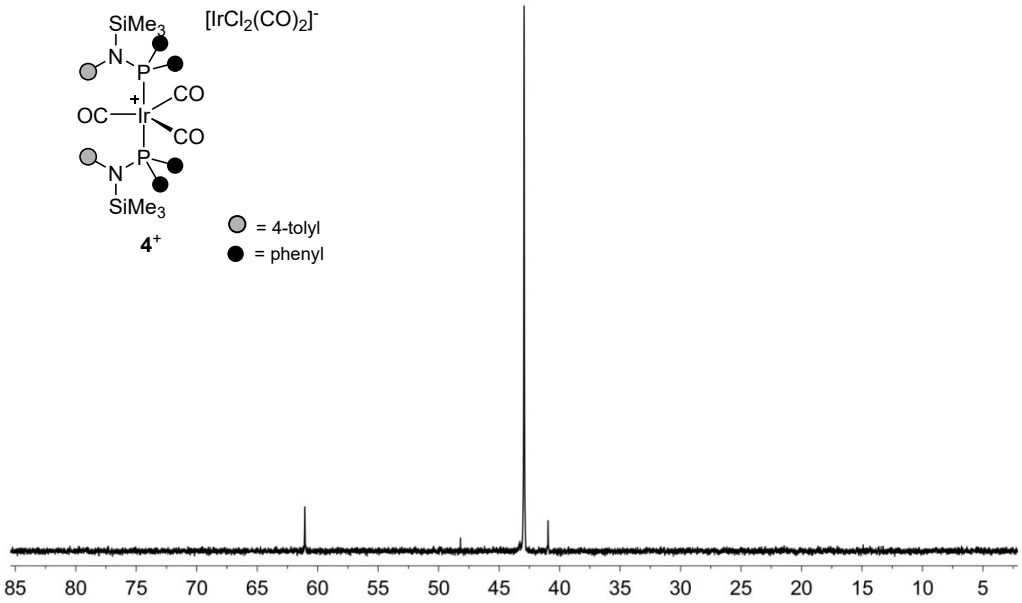

Fig. SI25. $^{31}P\{^{1}H\}$ NMR spectrum of 4.

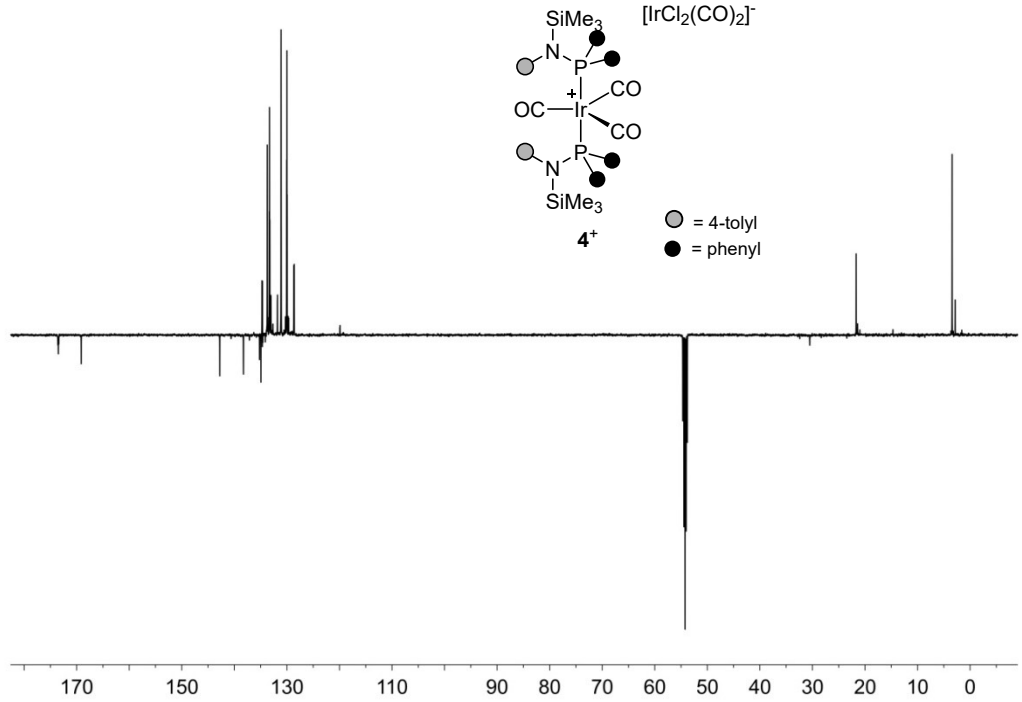

Fig. SI26. $^{13}C\{^{1}H\}$-apt NMR spectrum of **4**.

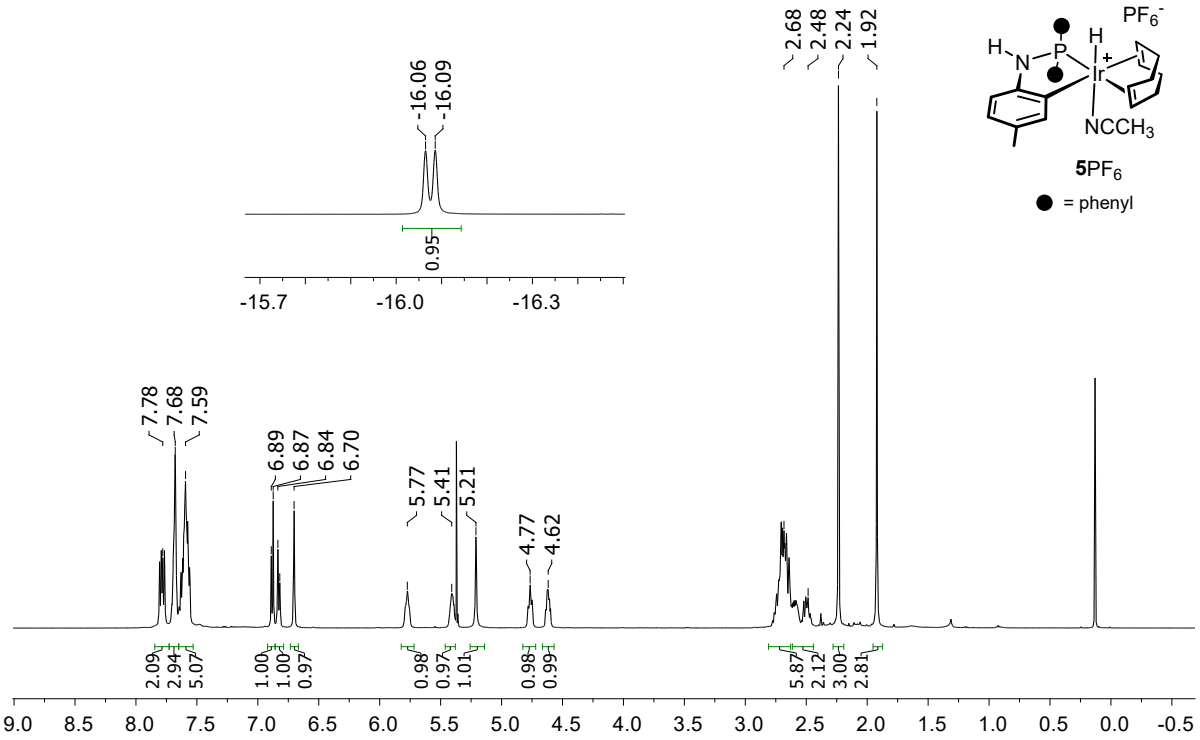

Fig. SI27. ^{1}H NMR spectrum of**5**PF_6.

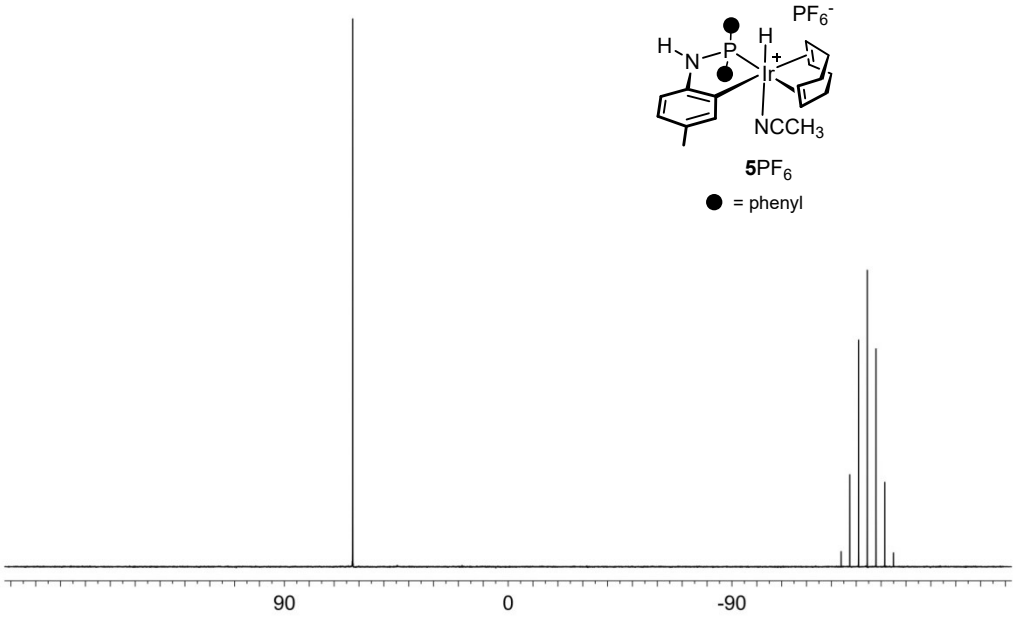

Fig. SI28. ^{31}P{^{1}H} NMR spectrum of**5**PF_6.

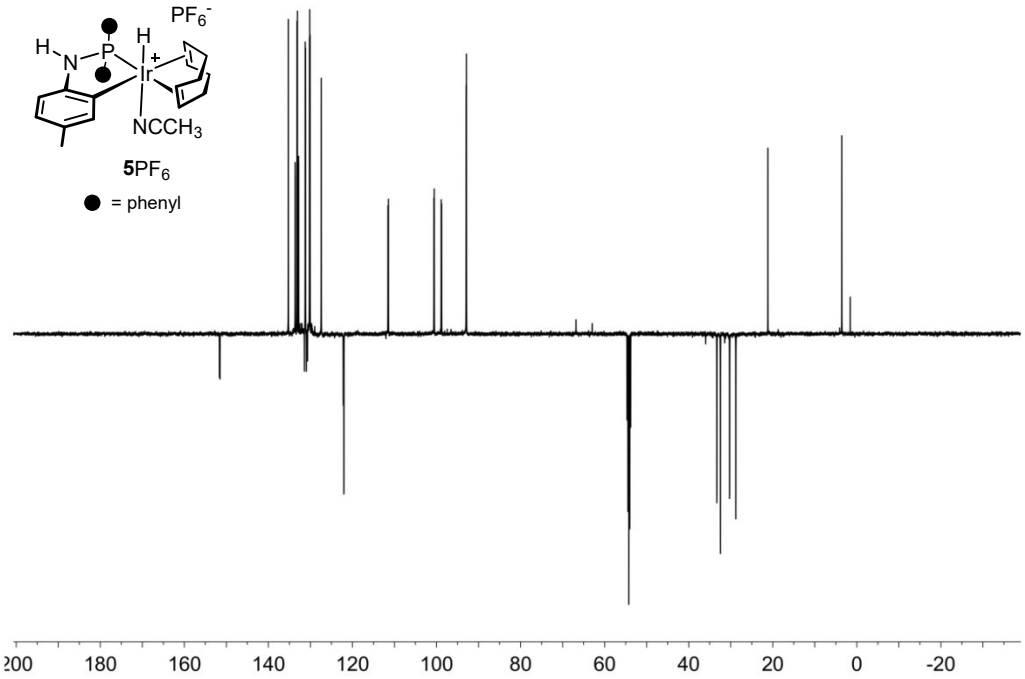

Fig. SI29. $^{13}C\{^{1}H\}$-apt NMR spectrum of **5**PF_6.

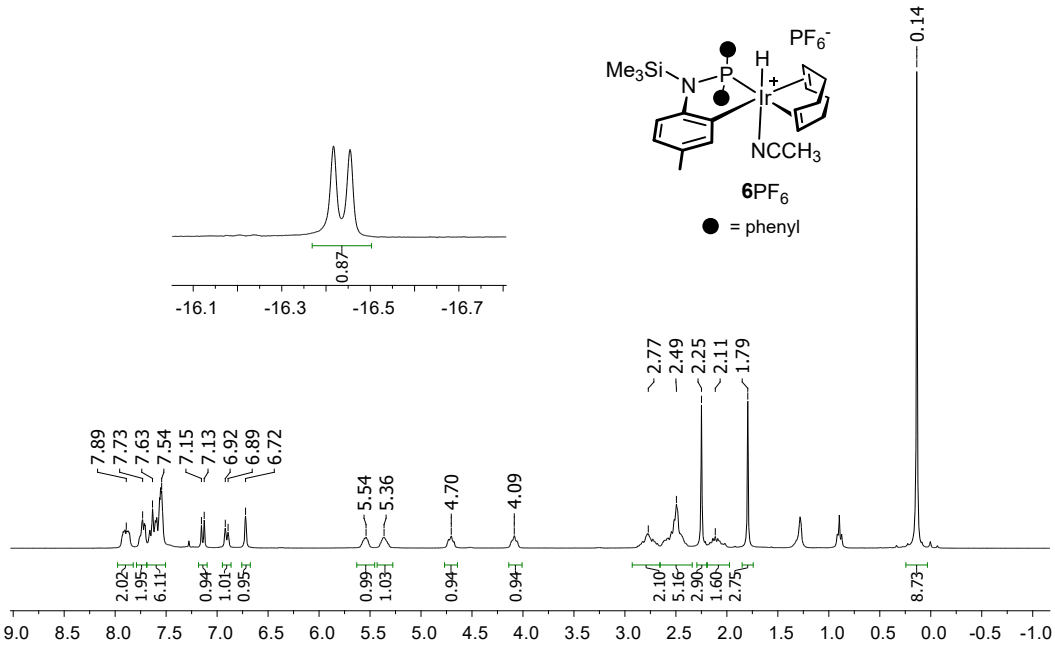

Fig. SI30. ^{1}H NMR spectrum of **6**PF_6.

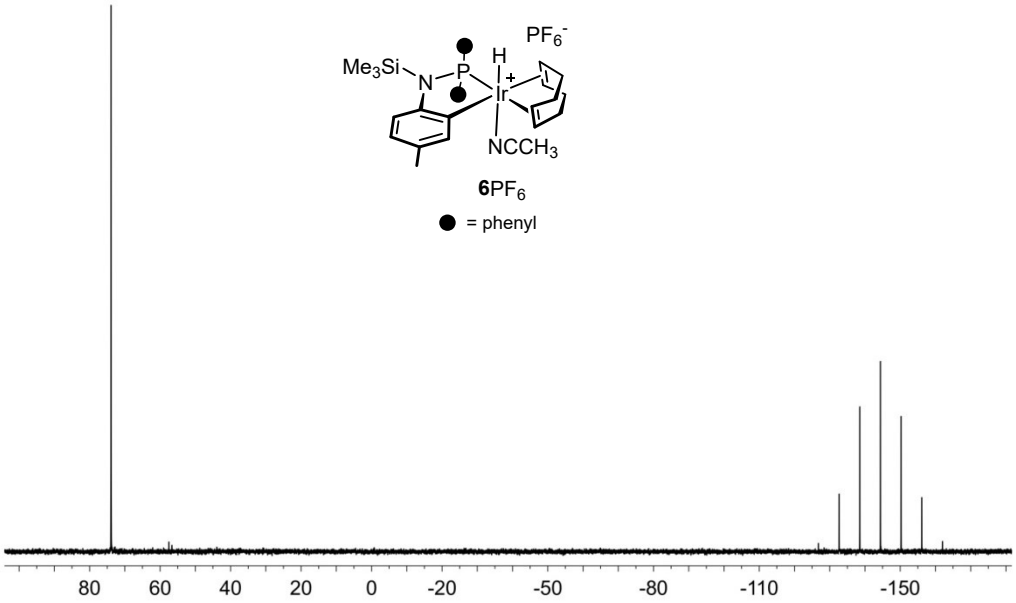

Fig. SI31. $^{31}P\{^{1}H\}$ NMR spectrum of **6**PF_6.

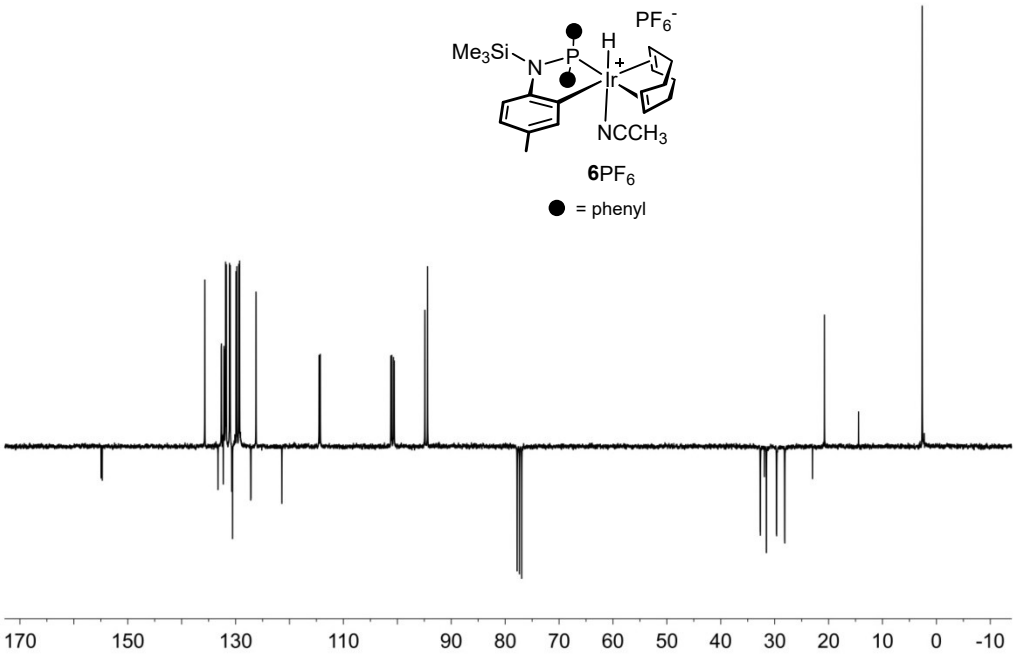

Fig. SI32. $^{13}C\{^{1}H\}$-apt NMR spectrum of **6**PF_6.

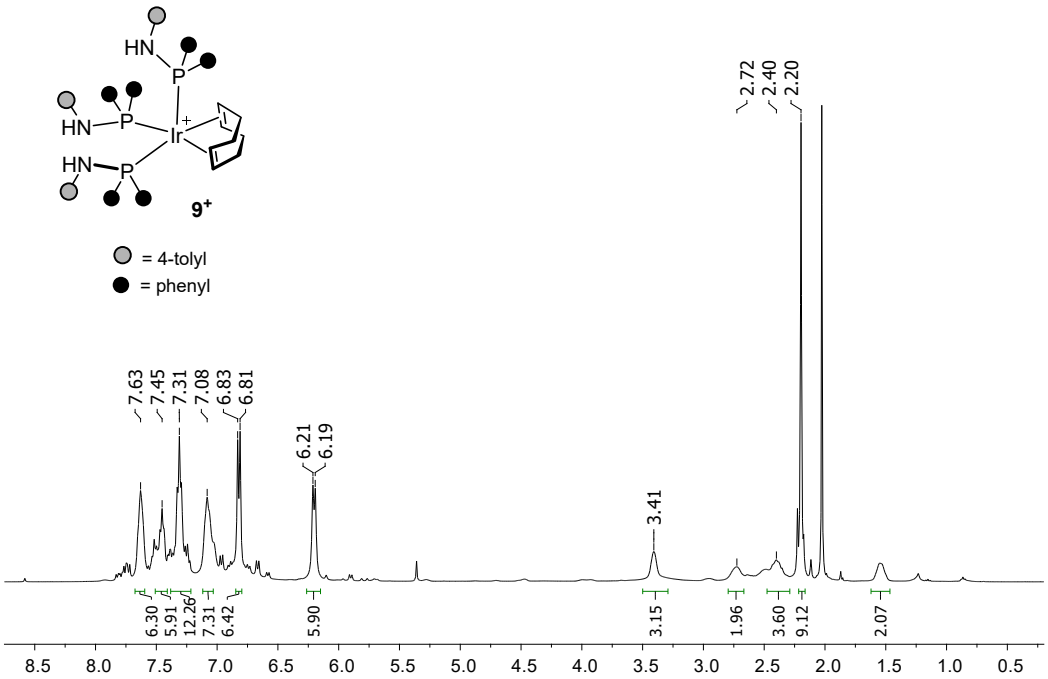

Fig. SI33. ^{1}H NMR spectrum of **9**$^{+}$ (233 K, CD_2Cl_2, prepared in situ).

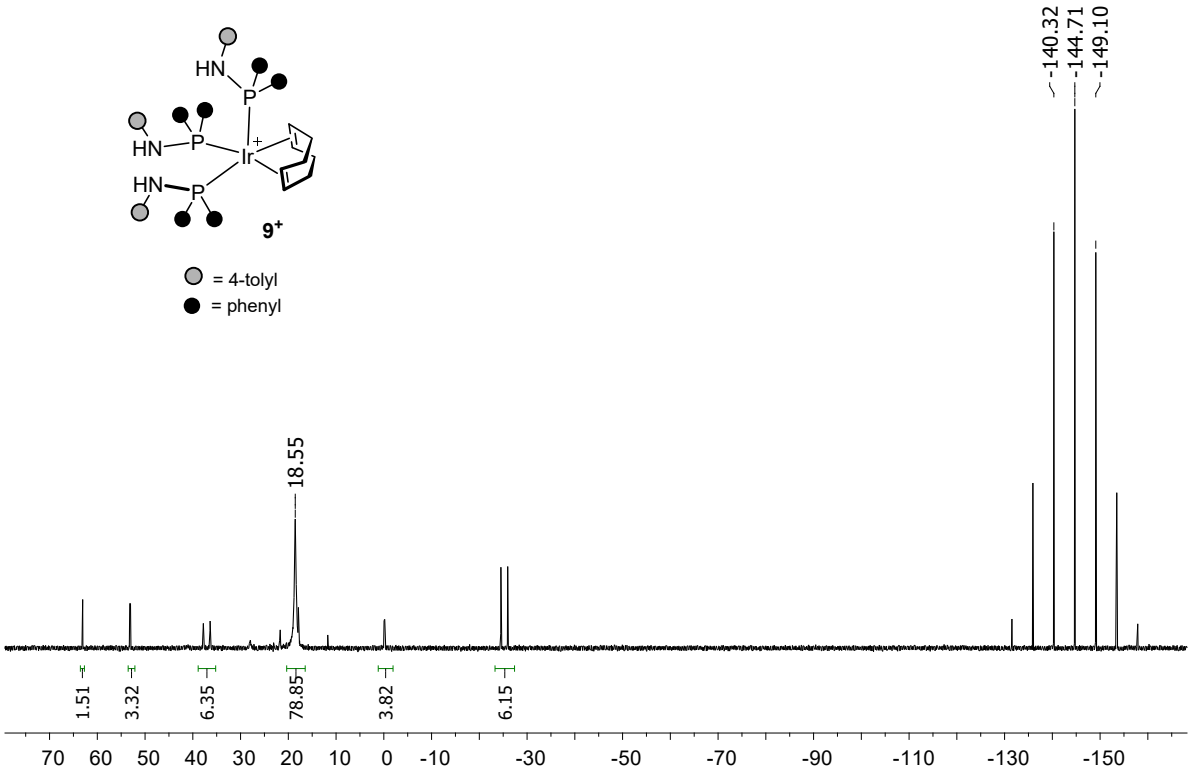

Fig. SI34. ^{31}P{^{1}H} NMR spectrum of **9**$^{+}$ (233 K, CD_2Cl_2, prepared in situ).

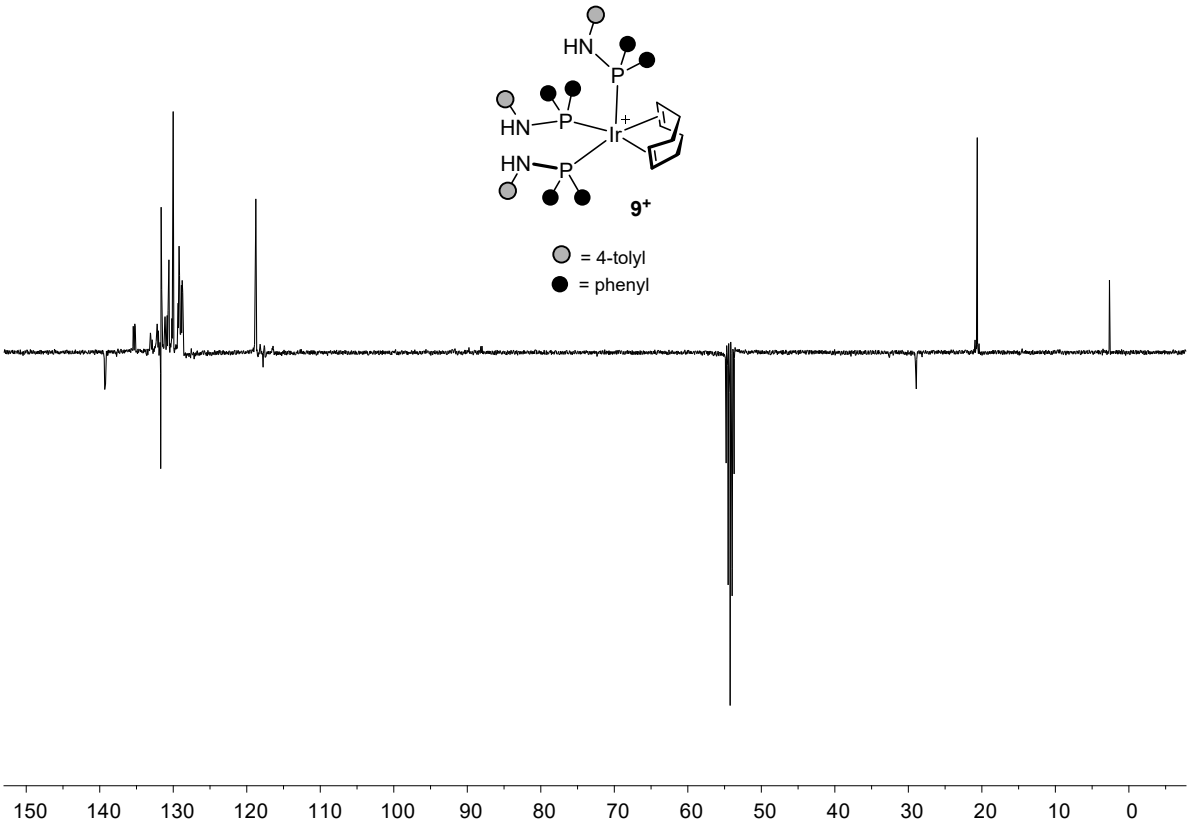

Fig. SI35. $^{13}C\{^{1}H\}$-apt NMR spectrum of **9**$^{+}$ (233 K, CD_2Cl_2, prepared in situ).

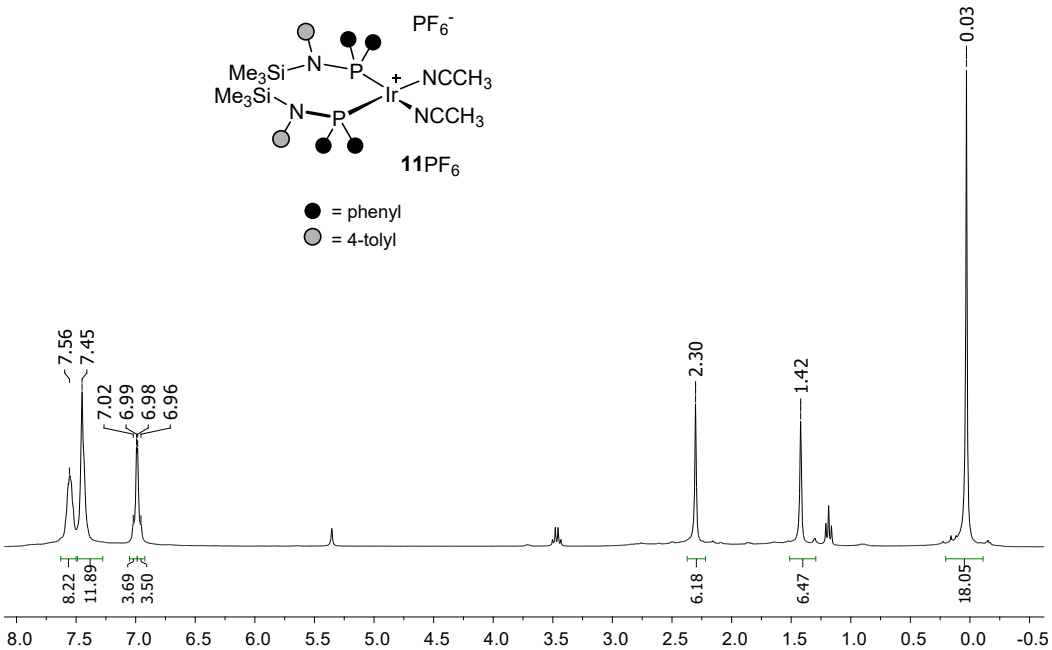

Fig. SI36. ^{1}H NMR spectrum of**11**PF_6.

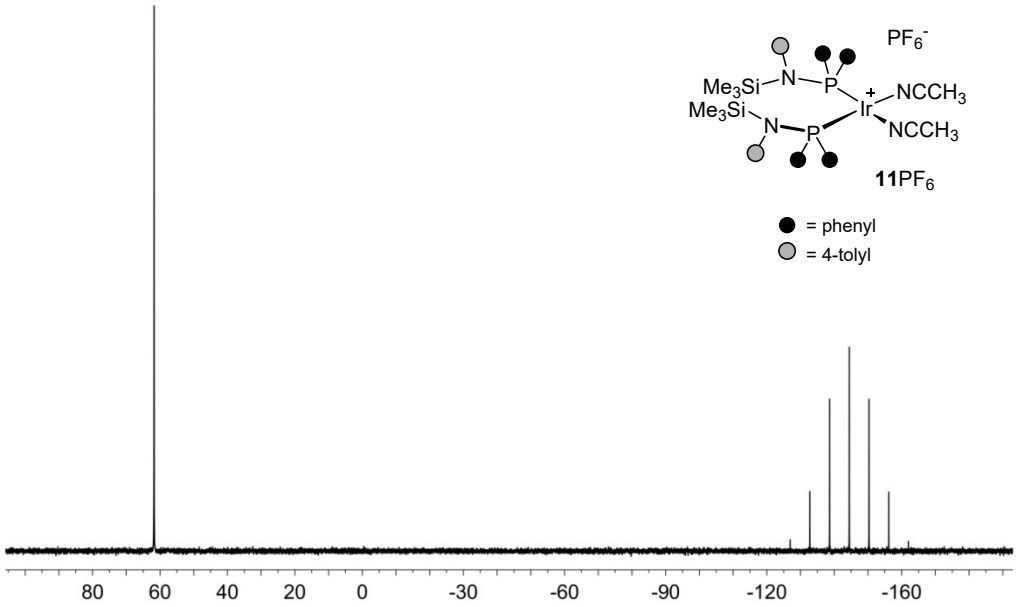

Fig. SI37. $^{31}P\{^{1}H\}$ NMR spectrum of **11**PF_6.

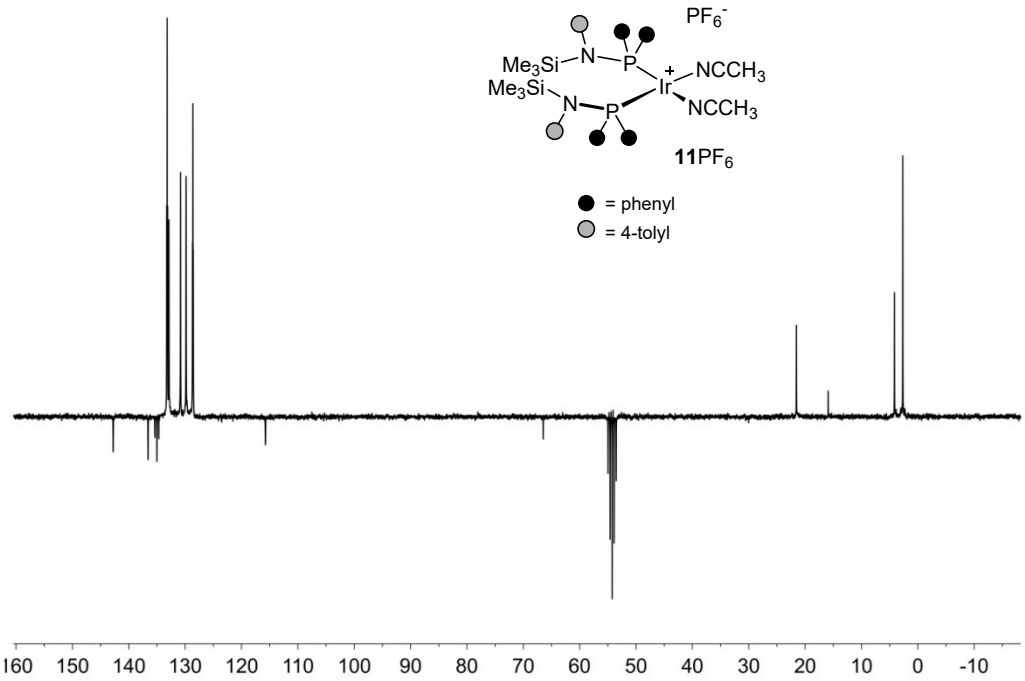

Fig. SI38. $^{13}C\{^{1}H\}$-apt NMR spectrum of **11**PF_6.

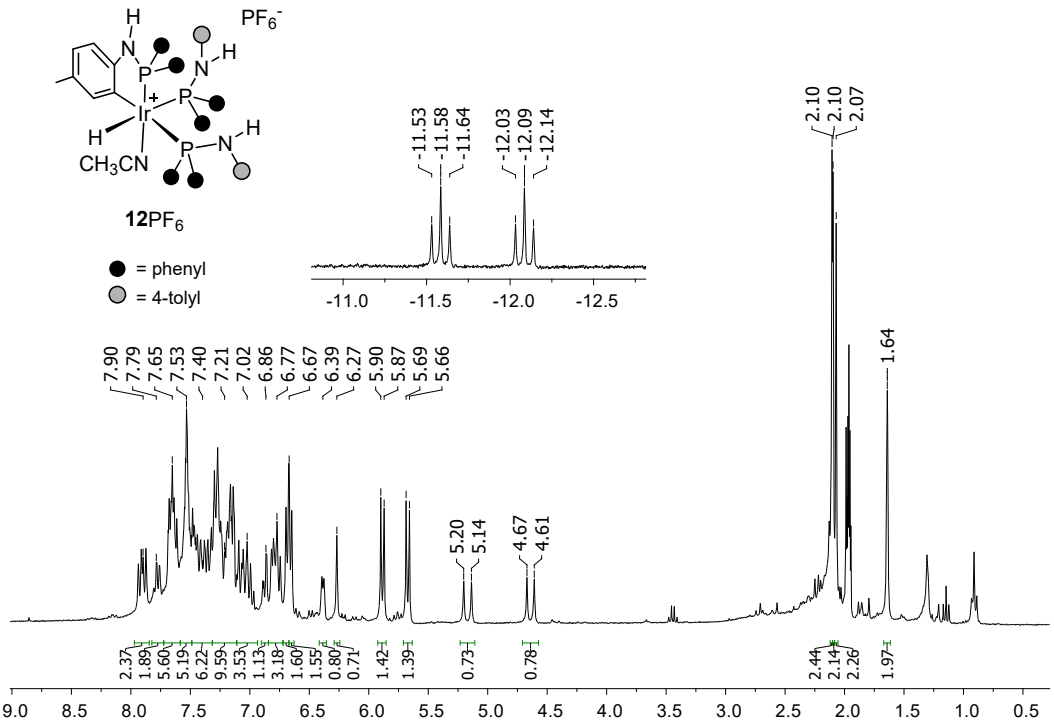

Fig. SI39. ^{1}H NMR spectrum of**12**PF_6.

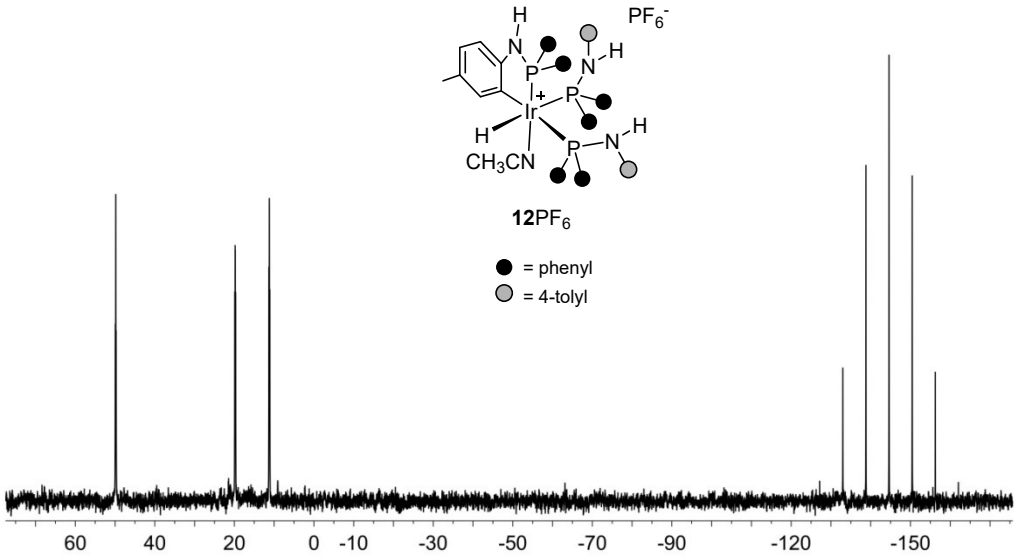

Fig. SI40. ^{31}P{^{1}H} NMR spectrum of **12**PF_6.

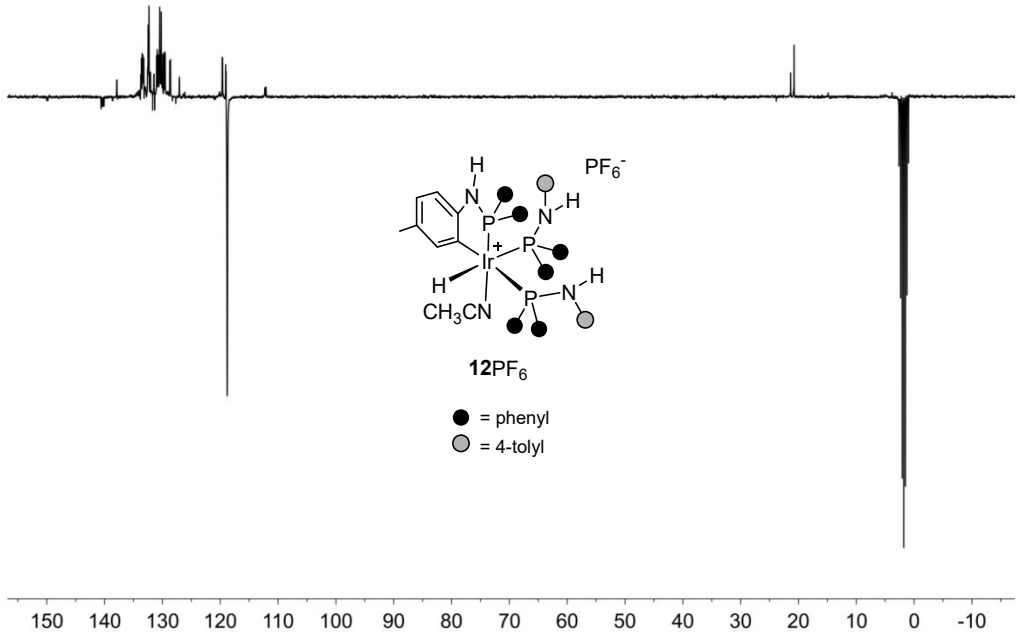

Fig. SI41. $^{13}C\{^{1}H\}$-apt NMR spectrum of **12**PF_6.

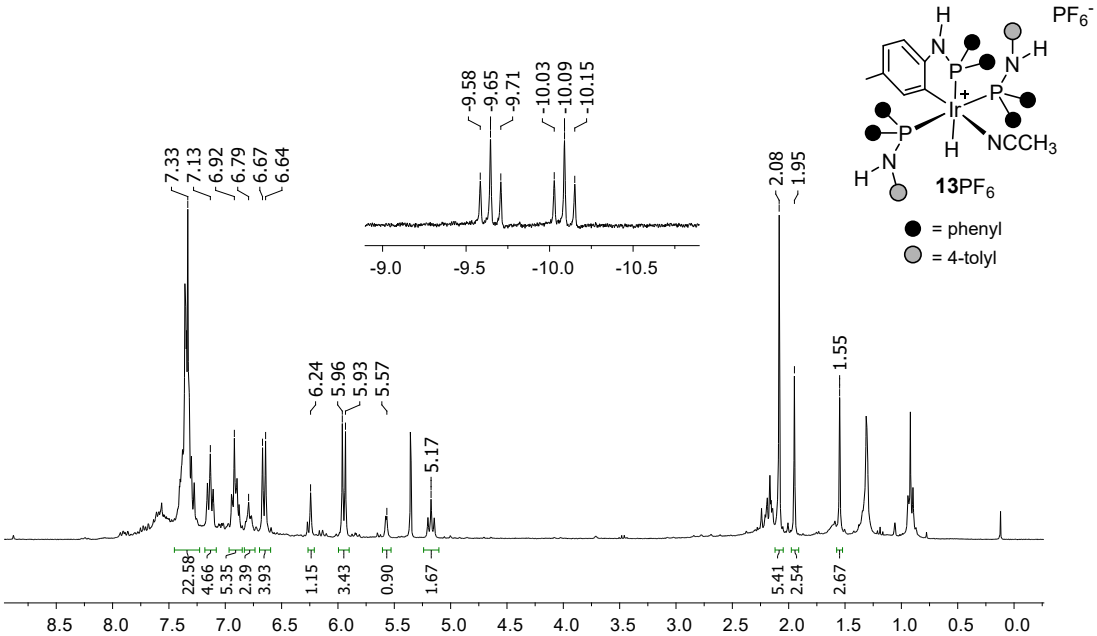

Fig. SI42. ^{1}H NMR spectrum of **13**PF_6.

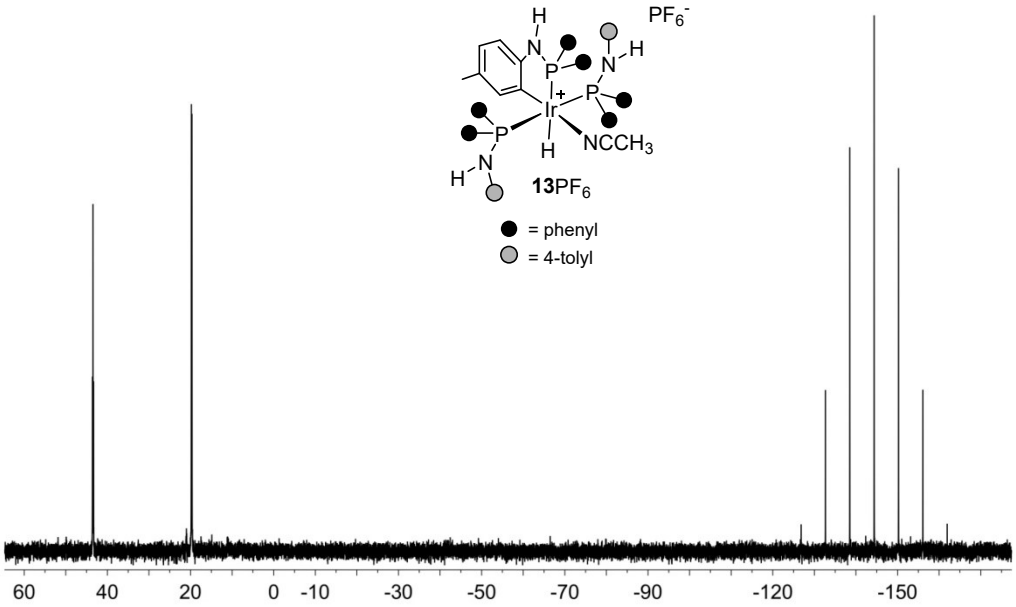

Fig. SI43. $^{31}P\{^{1}H\}$ NMR spectrum of **13**PF_6.

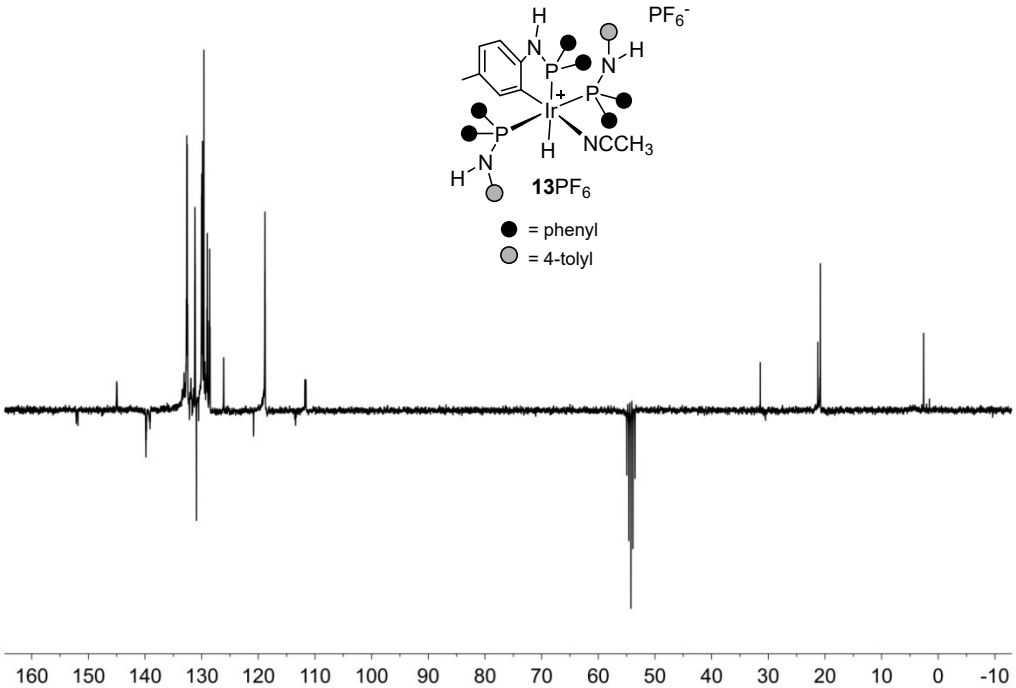

Fig. SI44. $^{13}C\{^{1}H\}$-apt NMR spectrum of **13**PF_6.

6. Monitoring of the reaction 12^+ ☐ 13^+ in CH_2Cl_2

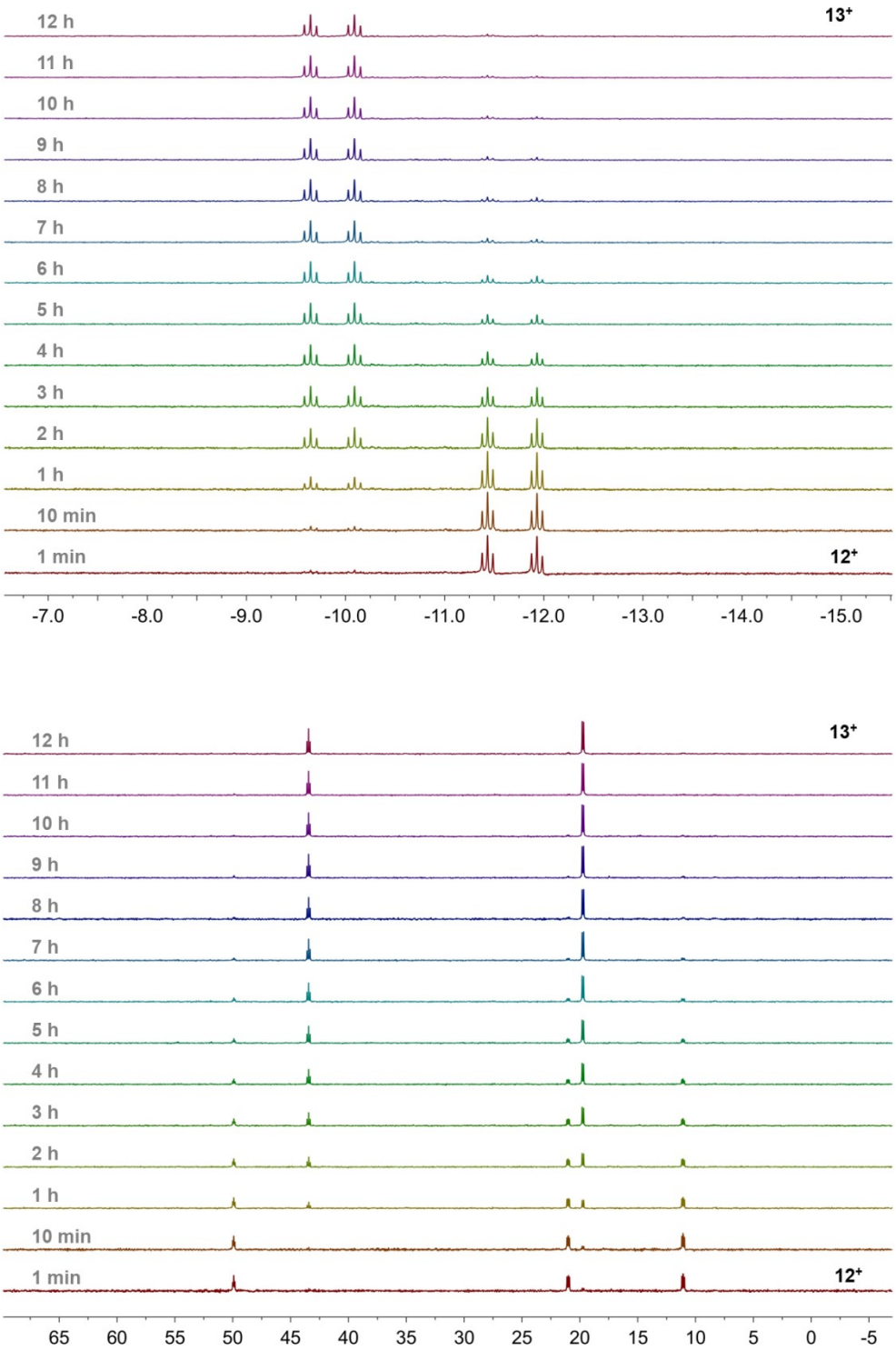

Fig. SI45. Monitoring of the reaction **12**$^+$ ☐ **13**$^+$ in CH_2Cl_2 at 298 K: (top) ^{1}H NMR; (bottom) ^{31}P{^{1}H} NMR.

7. DFT data for the reaction 7^+ ☐ 8^+

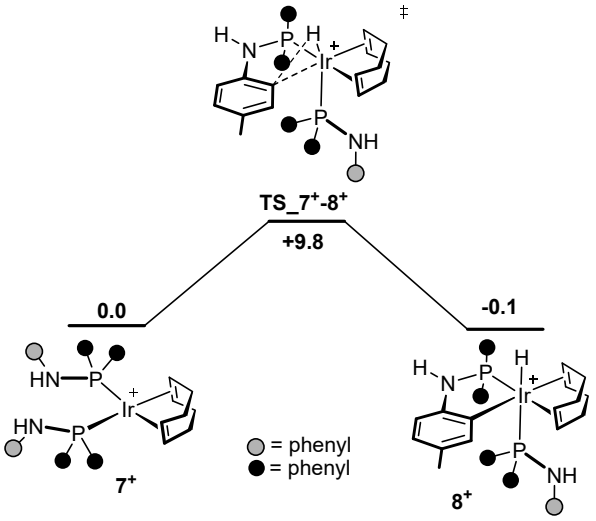

Fig. SI46. Gibbs free energy profile for the reaction 7^+ ☐ 8^+ along with the calculated Gibbs free energies (kcal·mol^{-1}, B3PW91-GD3BJ/def2svp, CH_2Cl_2, 298 K, 1 atm).